One-step electrochemical elaboration of SnO2 modified electrode for lead ion trace detection in drinking water using SWASV

Siham Lameche, Salah Eddine Berrabah, Abdelhakim Benchettara, Sabrina Tabti, Amar Manseri, Djaouida Djadi, Jean-François Bardeau

▶ **To cite this version:**

Siham Lameche, Salah Eddine Berrabah, Abdelhakim Benchettara, Sabrina Tabti, Amar Manseri, et al.. One-step electrochemical elaboration of SnO2 modified electrode for lead ion trace detection in drinking water using SWASV. Environmental Science and Pollution Research, 2023, 10.1007/s11356-023-25517-4 . hal-04015342

HAL Id: hal-04015342

https://univ-lemans.hal.science/hal-04015342

Submitted on 5 Mar 2023

HAL is a multi-disciplinary open access archive for the deposit and dissemination of scientific research documents, whether they are published or not. The documents may come from teaching and research institutions in France or abroad, or from public or private research centers.

L'archive ouverte pluridisciplinaire **HAL**, est destinée au dépôt et à la diffusion de documents scientifiques de niveau recherche, publiés ou non, émanant des établissements d'enseignement et de recherche français ou étrangers, des laboratoires publics ou privés.

Environmental Science and Pollution Research
https://doi.org/10.1007/s11356-023-25517-4

One-step electrochemical elaboration of SnO_2 modified electrode for lead ion trace detection in drinking water using SWASV

Siham Lameche[1] · Salah Eddine Berrabah[1] · Abdelhakim Benchettara[1] · Sabrina Tabti[1] · Amar Manseri[2] · Djaouida Djadi[1] · Jean-François Bardeau[3]

Abstract

A facile method was proposed for the elaboration of an electrochemical sensor for heavy metal's trace detection by using square wave anodic stripping voltammetry (SWASV); this method is based on a simple anodic conversion of tin electrode into Sn/SnO_2 modified electrode. Both electrochemical and physico-chemical techniques were used to confirm the modification process and better understand the electrode's behavior. Then, depending on the operating conditions, the response signal was studied and adjusted in order to obtain optimal sensor performance. When optimized, the proposed method reached a lowest detection limit (LOD) of 2.15 µg L^{-1} (0.0104 µM), and quantification limit (LOQ) of 5.36 µg L^{-1} (0.0259 µM), in linearity range between from 6.2 and 20.7 µg L^{-1}. Additionally, after having used the elaborated electrode for ten successive measurements, the repeatability remains very high with an RSD of approximately 5.3%; furthermore, ten other species appear to have very slight effect on Pb(II) detection. Finally, for the method validation, the proposed electrode was able to sense different lead concentration integrated in a local bottled spring water by showing recovery levels ranging from 103.8 to 108.4%.

Introduction

The presence of heavy metal ions (HMIs) in the environment, even in trace amounts, is dramatic because the toxicity of these pollutants disrupts ecosystems, deteriorates soil quality, and accumulates in the food chain, causing a major risk to human health (Jiang et al. 2019; Wu et al. 2019). It has been known for years that the discharge of wastewater from the paint and dye industry, metallurgy, and many other industries automatically leads to environmental pollution with the majority presence of Pb^{2+} (An et al. 2001) and that the contamination of the environment and soils by these heavy metals inexorably leads to their incorporation in drinking water and therefore in food, which explains this harmful effect (Masindi and Muedi 2018; Ackerman and Chang 2018).

The accumulation of lead Pb(II) in human blood can result in major complications such as: growth disorders, hyperactivity, learning problems, kidney damage, and anemia (Bai et al. 2022; Nodehi et al. 2022). The incidents in Flint (2014) and New York (2019), where lead levels were above 100 ppb and 50 ppb, respectively, have attracted public attention due to the occurrence of some lead poisoning cases in the area (Brennan et al. 2017). Since these events, the US Environmental Protection Agency has limited the permitted level of lead to 15 ppb in drinking water, and at this time, no alerts have been given on blood lead levels in young children (Dil and Sadeghi 2018). In small quantities, certain heavy metals such as Cu, Mn, Zn, and especially Fe are necessary for the human body (Vallee and Ulmer 1972), but other heavy metals such as As(III), Cd(II), Hg(II), and Pb(II) can in particular damage the nervous system or cause cancer.

✉ Salah Eddine Berrabah
se_berrabah@hotmail.com; sberrabah@usthb.dz

[1] Laboratory of Electrochemistry-Corrosion, Metallurgy and Mineral Chemistry, Faculty of Chemistry, USTHB, BP 32, 16111 Algiers, Algeria

[2] Research Center On Semiconductor Technology for Energetic (CRTSE), Thin Films Surface and Interface Division CMSI, 02 Bd. Frantz-Fanon, B.P. 140, Alger-7 Merveilles, Algiers, Algeria

[3] IMMM, Le Mans Université, UMR 6283 CNRS, Avenue Olivier Messiaen, 72085 Le Mans, France

The detection of Pb(II) ions by traditional analytical methods such as atomic absorption or emission spectros-copies (AAS, AES) (Hk 2016), inductively coupled plasma mass spectrometry (ICP-MS) (Bansod et al. 2017), and atomic fluorescence mass spectrometry (Corns et al. 2010) are expensive and require more or less difficult pretreatment processes.

In the last few years, new alternative technologies have been developed to allow the rapid detection of HMIs; among them, electrochemical detection methods stand out for their advantages: simplicity of use, high sensitivity, rapid detection, good selectivity, and high precision (Beitollahi et al. 2019; Safaei et al. 2019; Karimi-Maleh et al. 2022). These advan-tages can be fully exploited by the nature and structure of the sensor. Nanomaterials have been utilized in different applica-tion areas due to their particular physical and chemical char-acteristics. Baghayeri et al 2014 used a nanostructured carbon paste electrode for the detection of a pharmaceutical drug. Moreover, nanomaterials can also be used for the removal of organic pollutants (Sun et al. 2023; Golikand et al 2009).

Square wave anodic stripping voltammetry (SWASV) used for metal ion detection as an alternative to traditional spectroscopic methods is a simple and reliable analytical technique, inexpensive, fast, and suitable for field applica-tions (Bansod et al. 2017; Terbouche et al. 2016) superior in terms of sensitivity, reproducibility and accuracy (Alghamdi 2010). Its high sensitivity can be attributed to the pre-con-centration step (Nodehi et al. 2021). During this step, metals of the electrolyte are accumulated on the working electrode. Then, the electrode is swept linearly to positive potentials so that their metals, one at a time, are removed from the electrode and re-oxidized to a potential characteristic of each metal (Baghayeri et al. 2021).

Previously, anodic voltammetry of metal ions was per-formed on mercury-based electrodes (Phal et al. 2021), but due to their negative effects on the environment, many coun-tries have banned their use and it has become urgent to find other types of electrodes.

Recently, due to their low cost, compatibility, and high adsorption to HMIs (Gao et al. 2013; Aragay et al 2011), inorganic materials and in particular nanomaterial-based metals, carbonaceous metals and their composites as well as metal oxides have attracted considerable attention and have become most commonly used elements in the electro-chemical detection of HMIs (Kim et al. 2022; Abdul Hamid et al. 2021).

The 3.6-eV band gap of the n-type semiconductor SnO_2 makes it appropriate for usage in a variety of applications such as gas sensors, lithium-ion batteries, and superca-pacitors (Xu et al. 2013). SnO_2 nanoparticles with unique properties such as high electrical conductivity and chemical sensitivity (Zhang et al. 2015) have attracted the attention of many research groups to develop new types of electrochemical sensors (Song et al. 2011).

The objective of this work is to develop a simple electrochemical method allowing the detection of Pb(II). The Sn/SnO_2 modified electrode showed improved electron transfer properties compared to bare Sn. Therefore, such electrode was used to effectively detect lead in drinking water by anodic square wave voltammetry. Several electrochemical and physicochemical techniques were used for surface characterization, such as open circuit potential (OCP), electrochemical impedance spectroscopy (EIS), scanning electron microscope (FESEM), X-ray diffraction (XRD), and X-ray photoelectron spectroscopy (XPS). Then, several parameters were studied and optimized, including supporting electrolyte, pH, potential and deposition time, in order to obtain a higher signal for Pb(II) detection. The interference of other heavy metals and repeatability experiments were also conducted, and finally, the applicability was demonstrated by the determination of Pb(II) in real water samples.

Experimental details

Chemicals

All chemical substances employed in this work were of analytical grade. A sodium hydroxide NaOH with a purity of 99% (Fluka) was used as supporting electrolyte. Hydrogen chloride HCl with purity of 37% and density 1.19 (Sigma-Aldrich) was used for adjusting pH. The PBS buffer solution of sodium phosphate Na_2HPO_4 (MERCK 99.0%) and potassium dihydrogen phosphate KH_2PO_4 (MERCK 99.5%) was used as supporting electrolyte for the detection of Pb(II). The distilled water used for the preparation of all solutions has a pH of 6.65 and an electric conductivity of 31.1 µS m^{-1}. Tin electrode was purchase from Reine Metal company with a purity of 99.9%.

Apparatus

All experiments were carried-out at constant temperature 25 °C using a thermostatic bath; square wave anodic stripping voltammetry (SWASV), open circuit potential (OCP), chronoamperometry, cyclic voltammetry (CV), and electrochemical impedance spectroscopy (EIS) were performed using a Princeton Applied Research potentiostat model Versastat 3 instrument equipped with the Versa-Studio 2.50.3 software. The impedance data were analyzed by fitting to electrical equivalent circuits with the Zview 3.5 software. The electrochemical tests were carried out in a double-walled glass cell with conventional three-electrodes, where Sn electrode with surface of 0.5 cm^2 was

used as a working electrode, a saturated calomel electrode (SCE) filled with KCl as reference (XR 110, Radiometer), and a platinum plate as the counter electrode.

The morphology of the modified electrode was characterized by scanning electron microscope JEOL JSM-7610FPlus. The X-ray diffractogram was obtained using the Bruker D2 Phaser 2G X-ray diffractometer). The XPS analysis were performed using ESCALAB Xi^+ from Thermo Scientific highlighting a monochromatic Al K Alpha X-ray source (1486.68 eV).

Elaboration process of Sn/SnO_2 modified electrode

In order to determine the potential of tin dioxide elaboration, a cyclic voltammogram was recorded in a sodium hydroxide solution (0.1 M NaOH). The potential scan was performed in the anodic direction on a tin electrode of 0.5 cm^2 surface area. The cyclic voltammetry curve was recorded in a potential range from − 0.1 to 1.5 V/SCE, with a rate of 50 mV s^{-1}. Figure 1 shows two anodic peaks upon the oxidation of the tin electrode, and after reversing the potential, a shoulder and a reduction peak are obtained.

The surface oxidation was performed using a chronoamperometry technique in 0.1 M NaOH. SM 1 shows that the current decreases rapidly in the first second, due to the double-layer charging process. Then, the current stabilizes at a practically constant value (17.3 µA) (Tabti et al. 2022). The decrease of the current is due to the gradual covering of the Tin surface by Tin dioxide, while the constant of the current indicates the growth rate of the oxide film, which is controlled by a diffusion mechanism (Hu and Hsu 2008). In order to have reproducible results, the working electrode was polished (Mecapol Presi-type 2B), under water with sandpaper grits 1200/4000 (Silicon Carbide). Before each test, the polished samples were properly rinsed with distilled water.

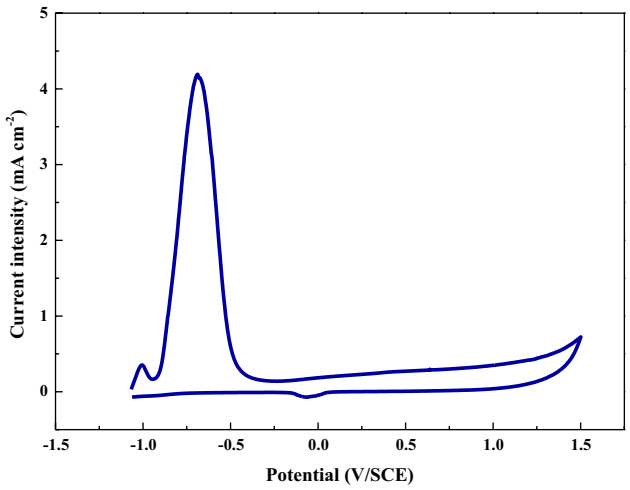

Fig. 1 Cyclic voltammogram of bare Sn in 0.1 M NaOH at scan rate of 50 mV s^{-1} at 25 °C

Results and discussion

Electrode characterization

Electrochemical characterizations

Electrochemical impedance spectroscopy (EIS) and open circuit potential (OCP) are effective methods for solid/liquid interface analysis. The comparison of the OCP of tin electrode before and after modification is a good tool to check the changes of surface state. According to SM 2, the anodic treatment of tin has ennobled the free potential confirming the modification process.

Furthermore, in order to properly study the electrochemical performance and the electron transfers properties of the bare and modified electrode materials, EIS tests were performed in PBS. The tests were performed at open circuit potential in the frequency range from 100 kHz to 0.01 Hz with an AC signal of 10 mV.

The corresponding Nyquist plots are presented in Fig. 2, the semicircle portion is corresponding to the electron-transfer resistance (Ret) at higher frequency range, while the linear part at lower frequency range represents the diffusion limited process (Wei et al. 2011; Brahimi et al. 2022). In Fig. 2, the semicircle diameter is gradually decreased at the modified electrode in comparison to bare tin electrode confirming a lower charge transfer resistance and higher electron transfer rate, consistent with the work of (Ziyatdinova et al. 2021), where they observed that the electron transfer resistance of glassy carbon modified with SnO_2 nanoparticles is 1.7 times lower than that of unmodified electrode. After data treatment (SM 4) with an appropriate equivalent circuit (inset Fig. 2), we can determine that the value of the double layer capacitance has decreased from 100 to 46.2 µF cm^{-2} after the anodique treatment and the formation of SnO_2, and the charge-transfer resistances have also decreased from 6719.41 to 335.4 Ω cm^{-2}. This result confirms the electrode modified with SnO_2 thin layer has better conductivity and faster electron transfer than the bare electrode (Liu et al. 2022).

SEM

To characterize the surface morphology of the modified electrode and compare its structure to the initial polished pure tin, Schottky-FEG scanning electron microscopy (SEM) observations were performed at different primary

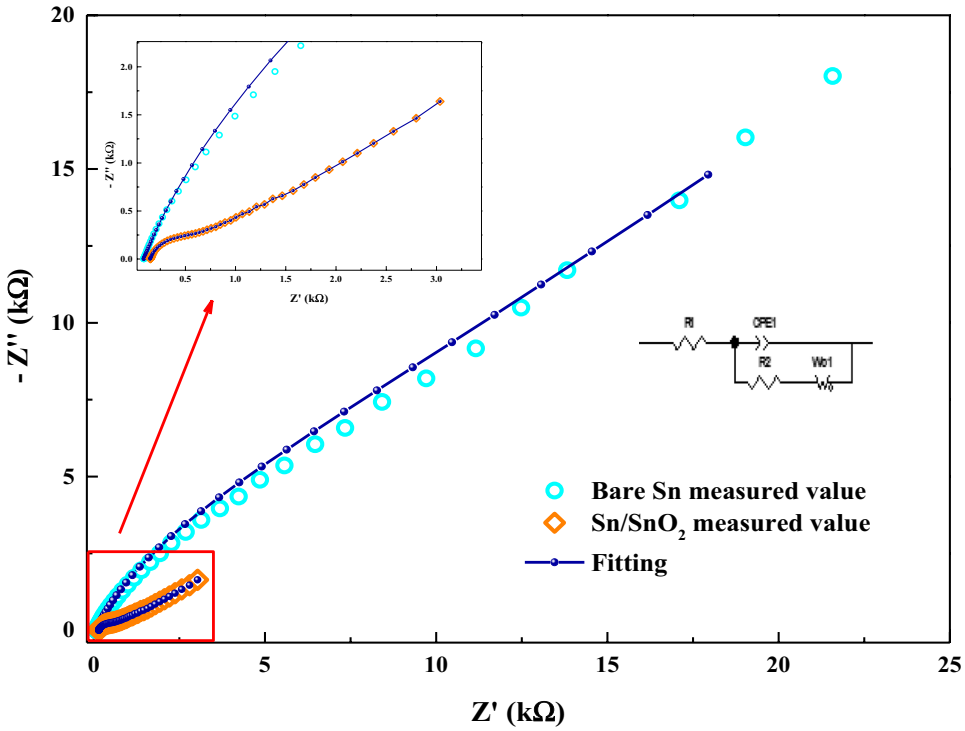

Fig. 2 Nyquist diagram of bare Sn and Sn/SnO_2 modified electrode with the corresponding fitting, inset: enlarged view of high-frequency semicircle and Randle's equivalent electrical circuit for the system

beam energies from 1 to 5 kV depending on the level of magnification. The micrographs in Fig. 3 show that after the oxidation process for 10 min, a thin nanoporous layer was formed on the electrode surface. To reveal this morphology, the beam deceleration mode (GB or Gentle Beam) was used to decrease the landing energy of primary electrons below 1 keV. By this mean, the volume effects were reduced (avoid detection of SEs and BSEs emerging from the depth tin substrate) and the contrast of the top-surface nanopores increased. This structure provides a large specific surface area and can hence have a positive effect on the detection capacity of the sensor (in particular by increasing the active surface of the electrode). SM 3 reveals that when the anodization time is extended up to one hour, a more compact layer is formed; however, this increase has no effect on the lead detection process; therefore, a 10-min process was sufficient to achieve maximum performance. Furthermore, the elemental mapping results (Fig. 3c and d) reveal that tin and oxygen elements are present and evenly distributed at the electrode surface.

XRD analysis

X-ray diffraction (XRD) analysis was used to study the crystallinity of modified electrode and to confirm the achievement of the desired phase after the anodic treatment. Figure 4 shows the observed pattern of the modified electrode. In addition to the substrate peaks (tin) that appear at $2\theta = 31°$, 32.31°, 44.24°, 45.2°, 55.63° (ICDD card no. 00–004-673) (Gurgul et al. 2020), new peaks assigned to tin dioxide (SnO_2) can be observed after 10 min of anodic treatment. These Bragg peaks which appear at $2\theta = 62.87°$, 64.89°, 72.66°, 73.41°, 79.76°, and 89.61° are successfully indexed to (221), (112), (202), (212), (321), and (312) diffraction planes of SnO_2 (ICSD # 880,287) which crystallize in the tetragonal system with the spacial group P $4_{2/m}$nm, confirming, therefore, the successful oxidation process and the crystallinity of the SnO_2 layer.

XPS analysis

The XPS analysis is an excellent analytical tool for elemental investigation, as the binding energy (BE) values of core levels are, to a certain extent, dependent on the molecular environment. Hence, the Sn/SnO_2 modified electrode was analyzed using XPS. All the XPS peaks were adjusted by referring the C1s binding energy (B.E.) to 284.6 eV.

Figure 5a depicts the XPS survey spectrum, which clearly shows the peaks of Sn, O, and C elements. The carbon could occur from pollution in the air or during the deposition process. The high resolution spectrums for the Sn3d and O1s regions are respectively shown in Fig. 5b and c. In Fig. 5b, two mirrored pair peaks were observed and centered at 486.2 eV and 494.7 eV which are corresponding to Sn $3d_{5/2}$ and Sn $3d_{3/2}$, respectively.

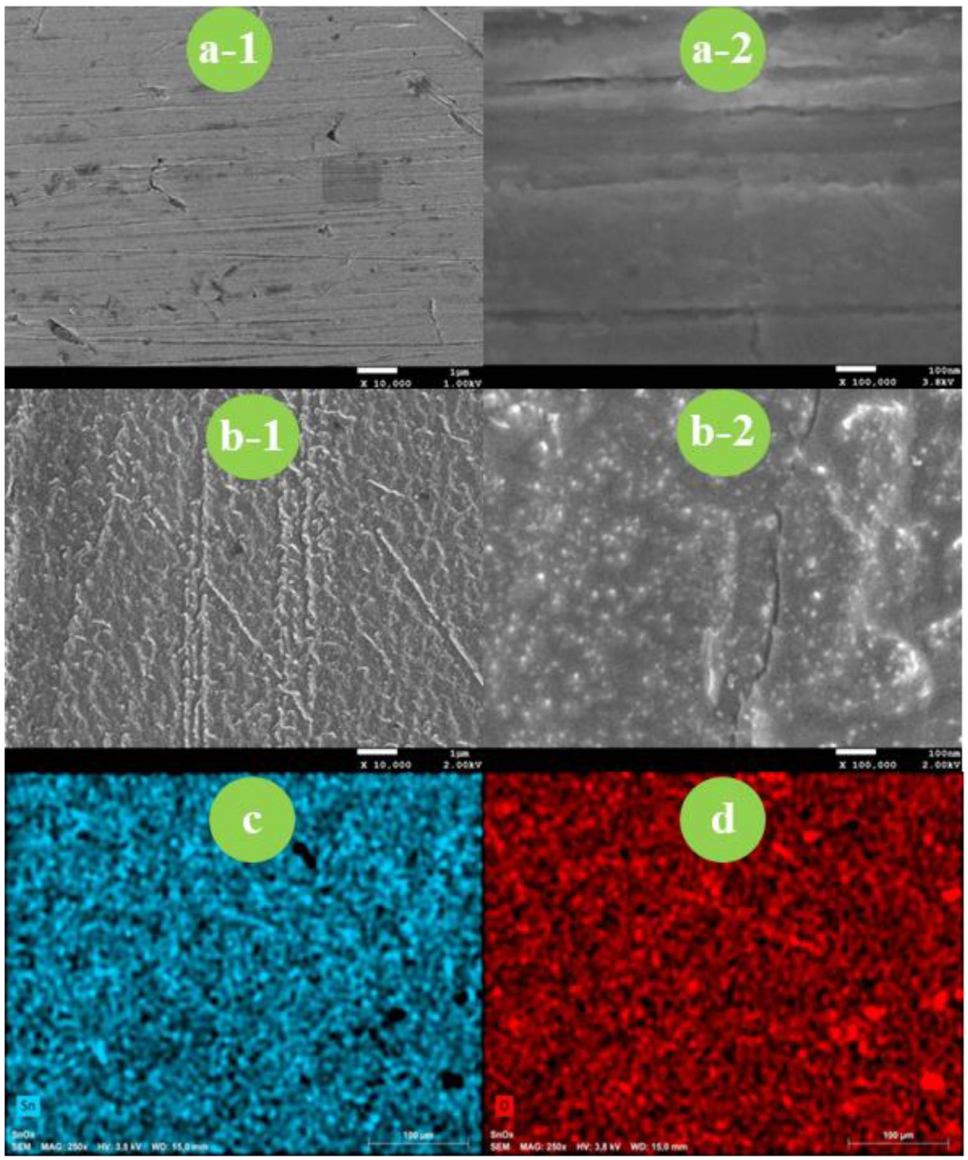

Fig. 3 FESEM images of Sn/SnO_2 modified electrode **a** before and **b** after 10 min of anodization; EDS elemental mapping of **c** tin and **d** oxygen

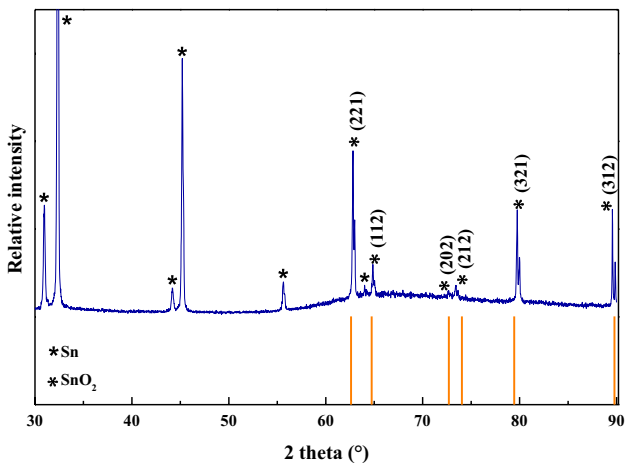

Fig. 4 X-ray diffractogram of Sn/SnO_2 modified electrode

There is a spin–orbit separation of 8.5 between the two peaks, which indicate that the Sn is in an oxidation state of + 4 (Babu et al. 2018; Suvith et al. 2020). Figure 5c depicts a wide non-symmetric curve of the O1s spectra, which has been fitted by two peaks having binding energies centered at 531.7 and 529.6 eV, which indicates the existence of two different oxygen species. Peak at 529.6 eV is commonly assigned to O^{2-} surface lattice oxygen, while the second peak at 531.7 eV is characteristic of oxygen adsorbed on the surface (O^{2-}, O^{-} etc.) (Liu et al. 2018; Mahieddine and Adnane-Amara 2023). The adsorbed oxygen is responsible for interacting with the external species, which enhances the SnO_2 performance in diverse applications such as molecules detection, photocatalytic efficiency, and CO_2 conversion (Vorokhta et al. 2018; Wang et al. 2019; Chen et al. 2019).

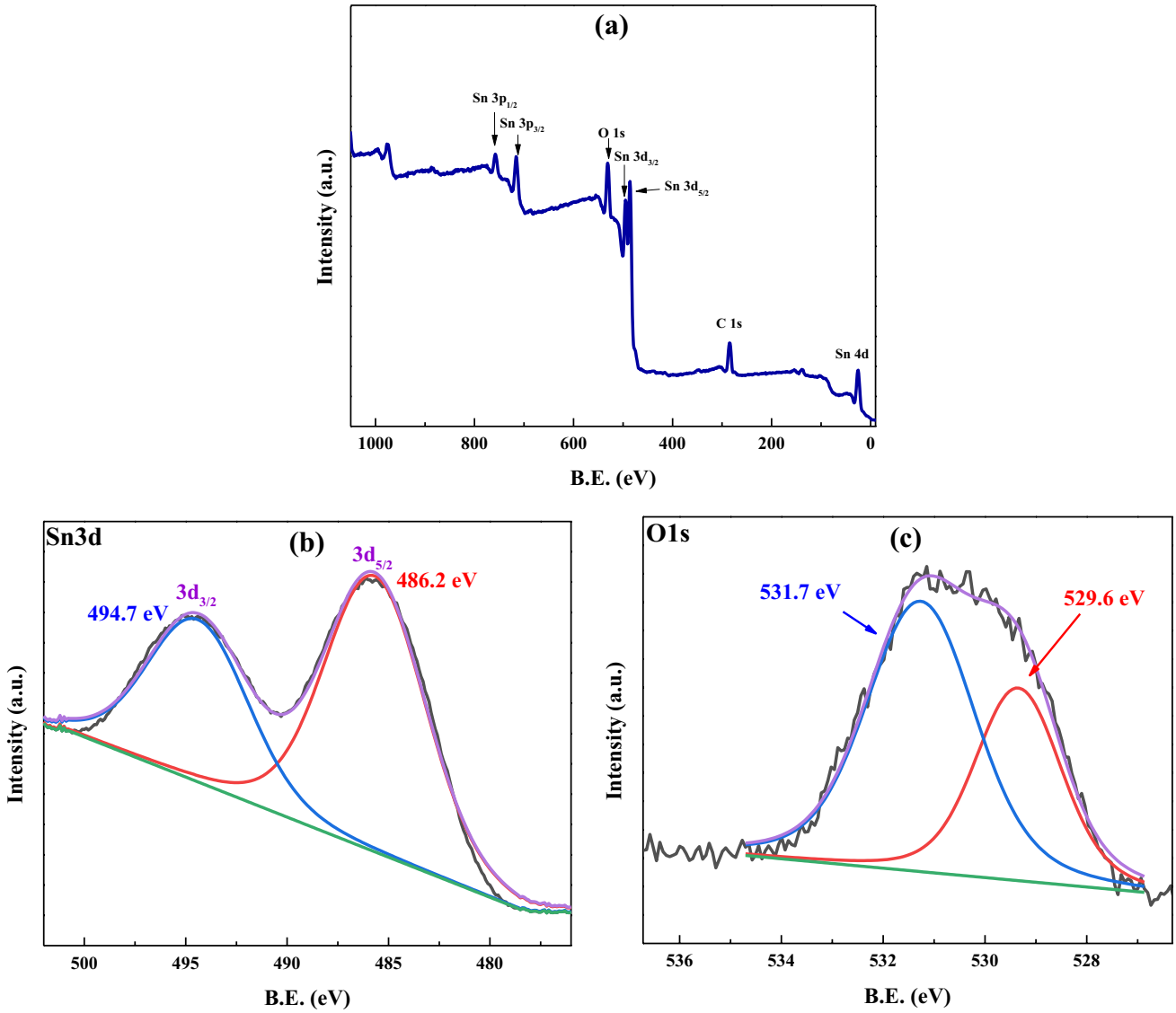

Fig. 5 XPS analysis of Sn/SnO_2. **a** The full survey spectrum; **b** Sn3d high-resolution spectrum; (**c**) O1s high-resolution spectrum

Lead detection by SWASV

In the detection of heavy metal, SWASV analysis has proven its effectiveness and remains favorable; its operating principle is based on redox reactions to generate a recorded current flow. The proposed mechanism for the detection of Pb^{2+} is illustrated in Scheme 1; it consists of two steps: electrochemical pre-concentration of heavy metals at a continuous potential onto the surface of the electrode. The targeted HMs ions (Pb^{2+}) we electroplated onto the surface of the sensor according to reaction 1, using a reduction potential of − 0.8 for 300 s under stirring. Then, it was left for 30 s to allow the solution to reach equilibrium

Reaction 1 : $Pb^{2+} + 2e^{-} \rightleftharpoons Pb^{0}$

The second step is the dissolution process, in which the deposited lead is removed (stripped) from the electrode surface and re-oxidized back into the solution according to the following reaction

Reaction 2 : $Pb^{0} \rightleftharpoons Pb^{2+} + 2e^{-}$

It can be seen that the modified electrode is able to generate a connection with more Pb(II) ions, due to its porous structure that creates more active sites for the selected ions.

The analytical performance of a given electrochemical sensor in stripping voltammetry methods is reflected in the height and shape of signal peak, which depend on various

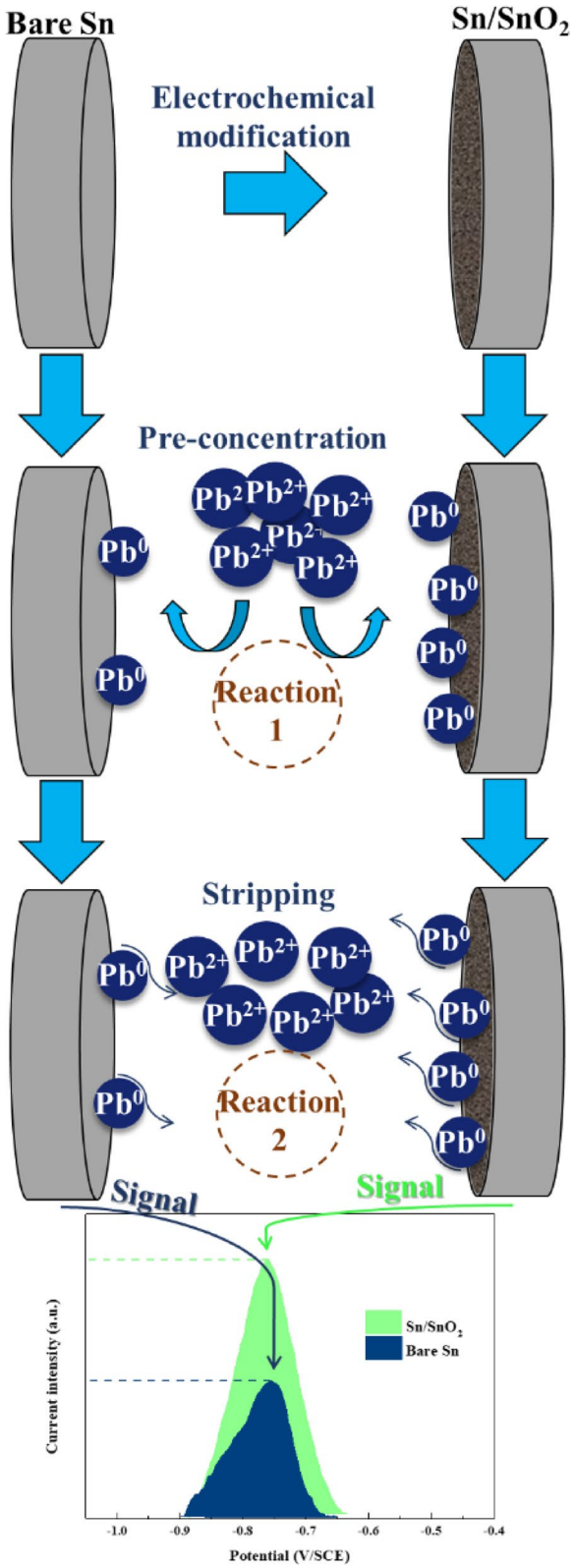

Scheme 1 The proposed mechanism for the detection of Pb(II) ions

parameters: (i) sensor-related parameters, i.e., sensitivity and nature of the selective electrode layer; (ii) technique-related parameters, such as, the supporting electrolyte, pH value, deposition potential, deposition time, frequency, pulse height, and step height. In the current study all these parameters were evaluated and optimized for Pb(II) detection.

Modification effect

In order to get an idea of the effect of the modification process, a square wave measurement was carried out at bare and modified electrode in PBS containing 20.7 µg L^{-1} of lead ions (Fig. 6). While a good response was register at bare Sn, it can be seen that it was significantly improved after oxidizing the tin electrode for 10 min and forming Sn/SnO_2, in which the current value was almost doubled, indicating that the modified electrode is almost 48% more efficient in lead sensing compared to bare tin electrode; this phenomenon is due to anodic treatment which creates cavities and increase of the active surface area of the electrode, confirming the findings

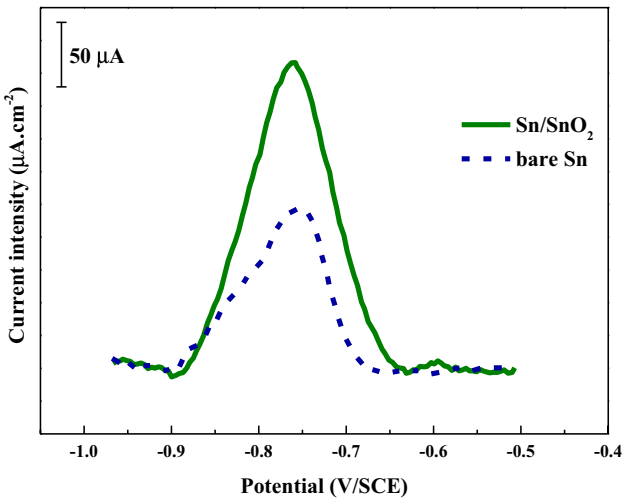

Fig. 6 Effect of modification process on Pb(II) SWASV signal at bare Sn electrode and Sn/SnO_2 modified electrode in PBS. Deposition potential: − 0.8 V, deposition time: 300 s, frequency: 50 Hz, pulse height: 40 mV, step height: 2 mV

obtained in the EIS results.

Effect of supporting electrolyte and pH

The effect of several supporting electrolytes were compared at Sn/SnO_2 modified electrode by adding 20.7 µg L^{-1} of Pb(II). In general, buffer solutions are widely used as an aqueous electrolyte solution because of their buffering properties that prevent large pH changes. Among Borax-HCl buffer solution (pH 8), phosphate buffer solution (pH 5.7), acetate buffer solution

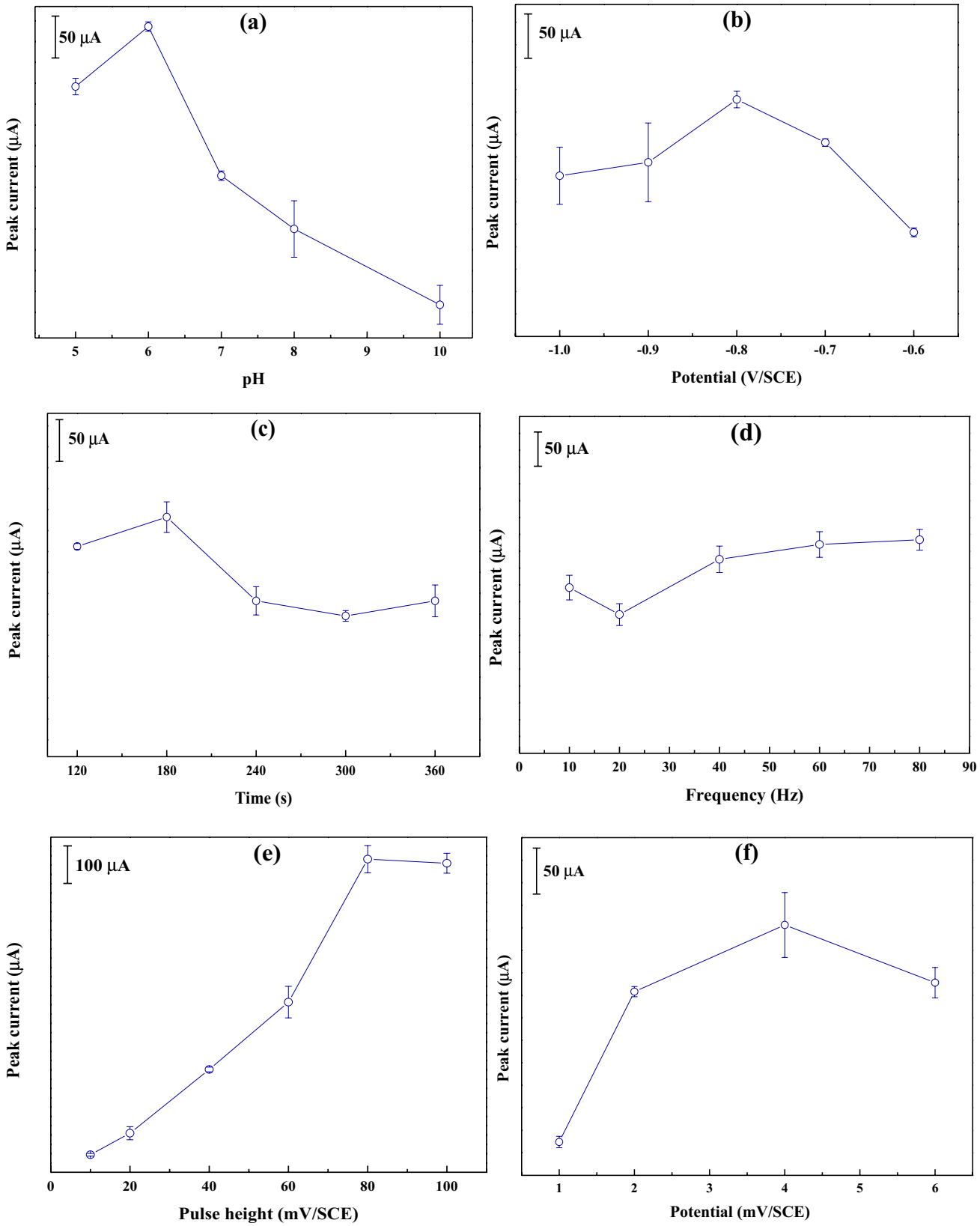

Fig. 7 Effect of **a** electrolyte pH from 5 to 10, **b** deposition potential from − 1.0 to − 0.6 V, **c** deposition time from 120 to 360 s, **d** SWASV frequency from 10 to 80 Hz, **e** SWASV pulse height from 10 to 100 mV, and **f** SWASV step height from 1 to 6 mV, on Pb(II) detection at Sn/SnO_2 modified electrode in PBS containing 20.7 µg $L.^{-1}$ of Pb(II)

(pH 4.6), and phosphate buffer solution (pH 7), the last one (PBS) provide the best shape and height of the peak; it was therefore chosen for all following experiments. Afterward, the pH effect was examined by varying the PBS pH from 5 to 10, and recording the response at 20 µg L^{-1} of Pb(II), As shown in Fig. 7a, the response (stripping peak current) is remarkably influenced by the pH values, where a common behavior was observed (Flores-Álvarez et al. 2021). Indeed, in basic solution (pH 8 and 10), Sn/SnO_2 does not show any adsorption capacity for Pb(II) by cationic exchange since the re-oxidation charge recorded is very weak which is due to hydrolysis of metals. On the other hand, in the acidic medium (pH 5 and lower) the Pb(II) metal ions compete with the protons of the solution for the active sites of the electrode, which minimizes the amount of metal deposited on the electrode, as the pH increases, the concentration of hydrogen ions decreases, consequently, the signal increases considerably until it reaches a maximum at pH 6 and then decreases at pH 7. Thus, the pH value of 6 was taken as the optimal.

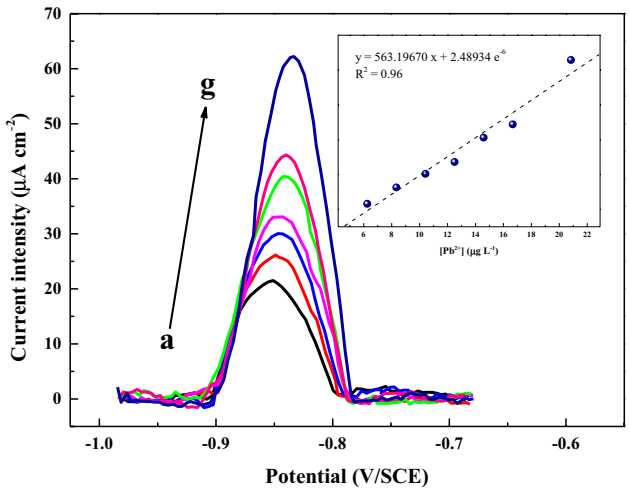

Fig. 8 SWASV curves of Pb(II) in PBS (pH 6) at concentration range from 6.2 to 20.7 µg L^{-1} under optimum conditions; deposition potential: − 0.8 V, deposition time: 120 s, frequency: 60 Hz, pulse height 80 mV and step height 4 mV, inset: calibration curve of Pb(II) detection

Efficiency of the pre-concentration step

The effect of deposition potential on peak intensity was studied in the range of − 1.0 to − 0.6 V at Sn/SnO_2 modified electrode (Fig. 7b). The importance of this parameter lays in its influence on the accumulation rate of the targeted ions. The curve shows that peak intensity increases when the potential value goes from − 0.6 to − 0.8 V until it reaches a maximum at this last value and then decreases at more positive values; at cathodic potentials, the hydrogen evolution became more and more important, creating bubbles at the electrode surface which prevent the reduction of lead, which reduce the current signals at extremely negative potentials.

Furthermore, the accumulation time impact on the peak current was studied between 120 and 360 s; the results are shown in Fig. 7c; it can be seen that as the deposition times increase, the signal response increases, indicating that more Pb(II) ions are accumulating and being absorbed at the electrode surface, which enhance the sensor sensitivity. However, after 180 s, the peak current started to decrease, indicating that saturation of the Pb(II) charge in the active sites on the electrode surface has occurred. As a result, the pre-concentration optimum conditions of Pb(II) was chosen as: potential: − 0.8 V, time: 180 s.

Optimization of the method parameters

The optimization of the instrumental parameters of the SWASV method (frequency, pulse and step heights) was also performed, starting from the frequency, in the range from 10 to 80 Hz

Table 1 Comparison of the analytical performance for electrochemical lead detection of other modified electrodes

Electrode	Technique	Linearity	LOD (µg L^{-1})	Ref
(PA/PPy)/ZIF-8@ZIF-67	DPV	4.14–41,440	0.6	Zhang et al. (2020)
BiFE-PLG	ASV	48.3–233	11.5	Bedin et al. (2018)
IJP-MW-CNT	SWASV	1036–5180	10.36	Rahm et al. (2020)
ErGO–MWNTs–L-cys	DPASV	41.44–8288	10.36	Al-Gahouari et al. (2020)
Fe_2O_3NPs/ ZnONRs/ ITO	SWASV	41.44–248.6	2.07	Hamid et al. (2021)
$MnFe_2O_4$/GO /GCE	SWASV	41.4–227.9	18.23	Zhou et al. (2018)
NiO/rGO/GCE	SWASV	-	2.07	Sun et al. (2019)
BiNP/Nafion/PGE	ASV	10–150	31.07	Palisoc et al. (2019)
$NH_2-Fe_3O_4$@C/ GCE	SWASV	165–2072	5.90	Bai et al. (2019)
polyPCA/GE	SWASV	40–1000	13.6	Dahaghin et al. (2021)
AOrGOC	SWASV	-	1.96	Kim et al. (2022)
Sn/SnO_2	SWASV	6.2–20.7	2.15	This work

(Fig. 7d), and the result shows that the peak current of Pb(II) increased with the increasing of the frequency and then slightly increased at frequency above 40 Hz. The pulse height effect was studied next in the range 10 to 100 mV; Fig. 7e shows that the peak current increased up to 80 mV, then maintained the same value at 100 mV. Finally, as shown in Fig. 7f, the step height produced the maximum current signal at 4 mV upon the variation from 1 to 6 mV. Thus, the optimal square wave parameters chosen for subsequent experiments were frequency of 60 Hz, pulse height of 80 mV, and step height of 4 mV.

Calibration curve and analytical performance

As described above, the optimization of the experimental parameters allows to find the ideal conditions for Pb(II) detection at Sn/SnO_2 modified electrode in PBS (pH 6) as supporting electrolyte. A current density vs lead concentration was obtained under the established conditions, as shown in Fig. 8 when lead concentration increase from 6.2 to 20.7 µg L^{-1}; the observed peaks are increasing, producing a linear relationship (calibration curve) between the current density and lead concentration (inset Fig. 8), the according correlation coefficient and regression equation are $R^2 = 0.96$ and $I_{Pb(II)}(A\ cm^{-2}) = 563.2\ x + 2.489e^{-6}$, respectively, where x represent the $[Pb^{2+}]$ in M. To access the analytical performance of an electrochemical sensor, the limit of detection (LOD) and the limit of quantification (LOQ) must be calculated, which is based on the calculation of the lowest concentration that the sensor can detect. The formulas used to calculate the detection and quantification limits of Pb(II) are the following.

$$\delta i_{LOD} = \overline{\delta i} + 3\sigma$$

$$\delta i_{LOQ} = \overline{\delta i} + 11\sigma$$

where $\overline{\delta i}$ is the average value of eleven times the blank signal and σ is the standard deviation between these measurements, δi_{LOD} and δi_{LOQ} are then replaced in the calibration curve equation, leading to a detection limit LOD of 2.15 µg L^{-1} (0.0104 µM) and a quantification limit LOQ of 5.36 µg L^{-1} (0.0259 µM). Which is comparable and in the most cases, lower than the LOD values obtained by several authors (Table 1).

Study of repeatability

Figure 9 show the repeatability capacity of the proposed sensor, which was studied via successive measurements ($n = 10$) without surface regeneration in PBS (pH 6) containing 20.7 µg L^{-1} of Pb(II) ions at the Sn/SnO_2 modified electrode. After each measurement, the working electrode was carefully polished to eliminate any adsorbed species using a chronoamperometry method,

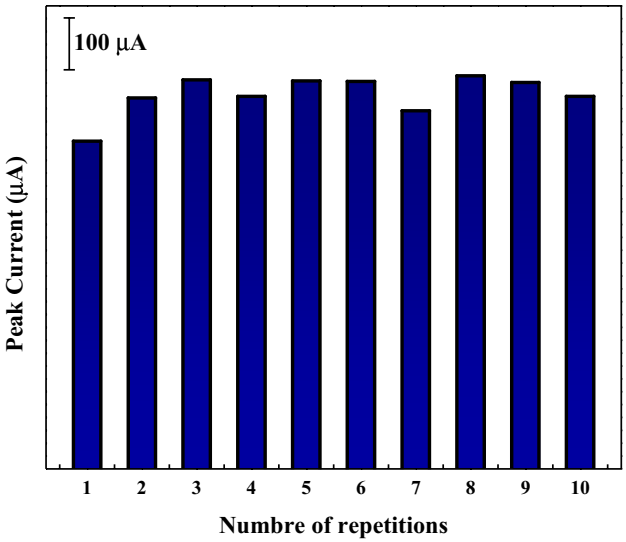

Fig. 9 Repeatability of Sn/SnO_2 in PBS (pH 6) containing 20.7 µg L^{-1} of Pb(II) under optimum conditions

a good relative standard deviations (RSD) of 5.28% was established, demonstrating the ability to use the Sn/SnO_2 modified electrode for multiple measurements with excellent precision.

Foreign ion effect

The interference study was performed under optimum conditions, in PBS (pH 6) containing 20.7 µg L^{-1} of Pb(II), by adding possible interfering ions of different nature and at different concentration, onefold (20.7 µg L^{-1}), 10 folds (207 µg L^{-1}), and 100 folds (2.07 mg L^{-1}). Ag(I), Ca(II), Cd(II), Co(II), Cu(II), Fe(II), Mg(II), Ni(II)m and Zn(II) were chosen due to their common presence in water sources.

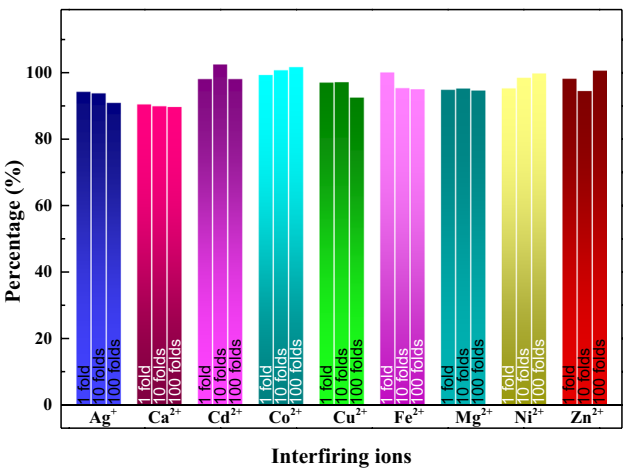

Fig. 10 Influence of interfering ions at Sn/SnO_2 modified electrode response to Pb(II) detection in PBS (pH 6) under optimum conditions

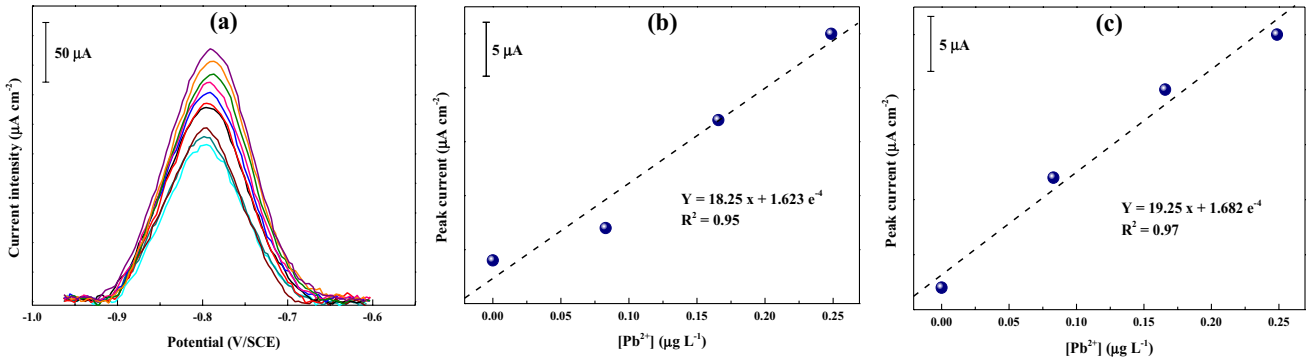

Fig. 11 Real sample analysis of Pb(II) from 1.24 to 2.28 mg L^{-1} in Ovitale bottled water with the corresponding regression equations and correlation coefficients

In order to assess the selectivity of the proposed method, the influence of each ion was evaluated by calculating the signal's percentage change with and without the foreign ions.

The ion interference is displayed in the histogram in Fig. 10, where it is obvious that, in all cases, no ion has an influence more than ± 10% on peak current even at very high concentrations (100 times Pb(II) concentration), suggesting that the presence of those ions had no effect on the electrode's selectivity, indicating the high selectivity of the proposed method.

Sensor validation

Standard addition method was used to assess the potential applicability of the Sn/SnO_2 modified electrode for the measurement of trace lead ions in drinking water samples. This method is commonly employed when the specific composition of the solution is unknown (Berrabah et al. 2021). The water chosen is a local bottled spring water Ovitale originating from the Kabyle mountains in the northeast of Algeria. The results achieved upon application of the proposed method using the electrochemical conditions optimized throughout this work are illustrated in Fig. 11; a founded concentrations of 1.8 and 1.808 mg L^{-1} were measured after the addition of 1.66 and 1.741 mg L^{-1} of Pb(II), suggesting recoveries of 108.4 and 103.8, respectively, which demonstrate the suitability of the Sn/SnO_2 modified electrode and the SWASV technique for the determination and detection of trace lead ions in in real aquatic environment and drinking water samples.

Conclusion

In the present study, a low-price electrochemical sensor was elaborated by a simple electrochemical conversion process based on tin modified electrode for ultra-sensing of lead ions in drinking water using SWASV. After investigating the effect of operation conditions on the response signal, an optimum performance of the elaborated sensor was achieved. Under ideal conditions, the proposed method displayed linear relationship between the currents and the Pb(II) concentrations in the range between 6.2 and 20.7 µg L^{-1} and a low limits of detection (LOD) and of quantification (LOQ) of 2.15 µg L^{-1} (0.0104 µM) and 5.36 µg L^{-1} (0.0259 µM), respectively, which is much lower than the World Health Organization WHO guideline of the maximum allowable lead concentration in drinking water which is 9.98704 µg L^{-1} (0.0482 µM). Additionally, the proposed method exhibited a good repeatability and a sensitive, accurate and rapid response towards Pb(II) ions, even in the presence of several interfering ions. The proposed sensor was validated for lead detection in drinking water samples with very satisfactory outcomes, which indicate its ability to be used for source water monitoring.

Supplementary Information The online version contains supplementary material available at https://doi.org/10.1007/s11356-023-25517-4.

Acknowledgements The authors wish to express their thanks for the Directorate General of Scientific Research and Technological Development (DGSRTD, Algiers). Also, we warmly thank Khaled DERKAOUI from Research Center of Semi-Conductor Technology for Energy, CRTSE, for his help in XPS analysis.

Author contribution Siham Lameche, writing, original draft preparation; Salah Eddine Berrabah, conceptualization, writing — review and editing, design; Abdelhakim Benchettara, literature survey; Sabrina Tabti, conceptualization; Amar Manseri, data analysis; Djaouida Djadi, visualization; Jean-François Bardeau, correction and supervision; all authors have read and agreed to the published version of the manuscript.

Funding This study was financially supported by the Faculty Chemistry (USTHB, Algiers).

References

Abdul Hamid H, Lockman Z, Mohamad N, Zakaria N, Abdul Razak K (2021) (2021) Sensitive detection of Pb ions by square wave anodic stripping voltammetry by using iron oxide nanoparticles decorated zinc oxide nanorods modified electrode. Mater Chem Phys 273:125148

Ackerman CM, Chang CJ (2018) Copper signaling in the brain and beyond. J Biol Chem 293(2018):4628–4635

Alghamdi AH (2010) (2010) Applications of stripping voltammetric techniques in food analysis. Arab J Chem 3(1):1–7

AL-Gahouari T, Bodkhe G, Sayyad P, Ingle N, Mahadik M, Shirsat SM, Deshmukh M, Musahwar N, Shirsat M (2020) Electrochemical sensor: L-cysteine induced selectivity enhancement of electrochemically reduced graphene oxide–multiwalled carbon nanotubes hybrid for detection of lead (Pb2+) ions. Front Mater 7:68. https://doi.org/10.3389/fmats.2020.00068

An HK, Park BY, Kim DS (2001) Crab shell for the removal of heavy metals from aqueous solution. Water Res 35(2001):3551–3556

Aragay G, Pons J, Merkoci A (2011) (2011) Recent trends in macro-, micro-, and nanomaterial-based tools and strategies for heavy-metal detection. Chem Rev 111(5):3433–3458

Babu B, Reddy IN, Yoo K, Kim D, Shim J (2018) Bandgap tuning and XPS study of SnO_2 quantum dots. Mat Let 221(2018):211–215

Baghayeri M, Amiri A, Karimabadi F et al (2021) Magnetic MWCNTs-dendrimer: a potential modifier for electrochemical evaluation of As (III) ions in real water samples. J Electroanal Chem 888(August 2020):115059. https://doi.org/10.1016/j.jelechem.2021.115059

Baghayeri M, Maleki B, Zarghani R (2014) Voltammetric behavior of tiopronin on carbon paste electrode modified with nanocrystalline Fe50Ni50 alloys. Mater Sci Eng C 44:175–182. https://doi.org/10.1016/j.msec.2014.08.023

Bai B, Bai F, Li X, Nie Q, Jia X, Wu H (2022) The remediation efficiency of heavy metal pollutants in water by industrial red mud particle waste. Environ Technol Innov 28:102944. https://doi.org/10.1016/j.eti.2022.102944

Bai F, Zhang X, Hou X, Liu H, Chen J, Yang T (2019) (2019) Individual and simultaneous voltammetric determination of Cd(II), Cu(II) and Pb(II) applying amino functionalized Fe3O4@carbon microspheres modified electrode. Electroanalysis 31(8):1448–1457

Bansod B, Kumar T, Thakur R, Rana S, Singh I (2017) A review on various electrochemical techniques for heavy metal ions detection with different sensing platforms. Biosens Bioelectron 94(2017):443–445

Bedin KC, Mitsuyasu EY, Ronix A, Cazetta AL, Pezoti O, Almeida VC (2018) Inexpensive bismuth-film electrode supported on pencil-lead graphite for determination of Pb(II) and Cd(II) ions by anodic stripping voltammetry. Int J Anal Chem 2018:1–9

Beitollahi H, Safaei M, Shishehbore MR, Tajik S (2019) (2019) Application of Fe3O4@SiO2/ GO nanocomposite for sensitive and selective electrochemical sensing of tryptophan. Electrochem Sci Eng 9(1):45–53

Berrabah SE, Benchettara A, Smaili F, Tabti S, and Benchettara A, (2021) Electrodeposition of zinc hydroxide on carbon graphite electrode for electrochemical determination of trace copper in water samples using square wave anodic stripping voltammetry. Mater Chem Phys 278(October 2021):125670, 2021

Brahimi B, Mekatel E, Kenfoud H, Berrabah SE, Trari M (2022) Efficient removal of the antibiotic Cefixime on $Mg_{0.3}Zn_{0.7}O$ under solar light: kinetic and mechanism studies. Environ Sci Pollut Res 29(50):75512–75524. https://doi.org/10.1007/s11356-022-20626-y

Brennan JT, Ogbonnewo I, Ogunleye O, Hernandez C, (2017) The standards for water quality testing: protecting the public from another Flint water crisis.

Chen Z, Fan T, Zhang YQ, Xiao J, Gao M, Duan N, Zhanga J, Li J, Liu Q, Yi X, Luo J-L (2019) Wavy SnO_2 catalyzed simultaneous reinforcement of carbon dioxide adsorption and activation towards electrochemical conversion of CO_2 to HCOOH. Apl Catlys b: Env 261(2019):118243

Corns WT, Chen B, Stockwell PB (2010) Atomic fluorescence spectrometry: a suitable detection technique in speciation studies for arsenic, selenium, antimony and mercury. J Anal at Spectrom 25(2010):933–946

Dahaghin Z, Kilmartin PA, Mousavi HZ (2021) 2021) A novel electrochemical sensor for simultaneous determination of cadmium and lead using graphite electrodes modified with poly(p-coumaric acid. Microchem J 168:106406

Dil NN, Sadeghi M (2018) Free radical synthesis of nanosilver/gelatin-poly (acrylic acid) nanocomposite hydrogels employed for antibacterial activity and removal of Cu (II) metal ions. J Hazard Mater 351(2018):38–53

Flores-Álvarez JM, Cortés-Arriagada D, Reyes-Gómez J, Gómez-Sandoval Z, Rojas-Montes JC, Pineda-Urbina K (2021) 2-Mercaptobenzothiazole modified carbon paste electrode as a novel copper sensor: an electrochemical and computational study. J Electroanal Chem 888(January). https://doi.org/10.1016/j.jelechem.2021.115208

Gao C, Yu XY, Xiong SQ, Liu JH, Huang XJ (2013) (2013) Electrochemical detection of arsenic(III) completely free from noble metal: Fe3O4 microspheres-room temperature ionic liquid composite showing better performance than gold. Anal Chem 85(5):2673–2680

Golikand AN, Raoof J, Baghayeri M, Asgari M, Irannejad L (2009) Nickel electrode modified by N, N-bis(salicylidene)phenylenediamine (Salophen) as a catalyst for methanol oxidation in alkaline medium. Russ J Electrochem 45(2):192–198. https://doi.org/10.1134/S1023193509020104

Gurgul M, Lytvynenko AS, Jarosz M, Gawlak K, Sulka GD, Zaraska L (2020) (2020) Hierarchical nanoporous Sn/SnOx systems obtained by anodic oxidation of electrochemically deposited Sn nanofoams. Nanomaterials 10(3):1–12

Hamid HA, Lockman Z, Mohamad Nor N, Zakaria ND, Abdul Razak K (2021) (2021) Sensitive detection of Pb ions by square wave anodic stripping voltammetry by using iron oxide nanoparticles decorated zinc oxide nanorods modified electrode. Mater Chem Phys 273:125148

Hk T (2016) (2016) Atomic absorption spectroscopic determination of heavy metal concentrations in Kulufo River, Arbaminch, Gamo Gofa, Ethiopia. J Environ Anal Chem 03(01):1–4

Hu CC, Hsu TY (2008) Effects of complex agents on the anodic deposition and electrochemical characteristics of cobalt oxides. Electrochim Acta 53(2008):2386–2395

Jiang Y, Liu C, Huang A (2019) (2019) EDTA-functionalized covalent organic framework for the removal of heavy-metal ions. ACS Appl Mater Interfaces 11(35):32186–32191

Karimi-Maleh H, Beitollahi H, Senthil Kumar P et al (2022) Recent advances in carbon nanomaterials-based electrochemical sensors for food azo dyes detection. Food Chem Toxicol 164(February). https://doi.org/10.1016/j.fct.2022.112961

Kim C, Park J, Kim W, Lee W, Na S, Park J (2022) (2022) Detection of Cd^{2+} and Pb^{2+} using amyloid oligomer–reduced graphene oxide composite. Bioelectrochemistry 147:108214

Liu D, Pan J, Tang J, Liu W, Bai S, Luo R (2018) Ag decorated SnO_2 nanoparticles to enhance formaldehyde sensing properties. Jrnl Phys Chem of Soli 124(2018):36–43

Liu Z, Wang R, Xue Q, Chang C, Liu Y, He L (2023) Highly efficient detection of Cd(II) ions in water by graphitic carbon nitride and tin dioxide nanoparticles modified glassy carbon electrode. Inorg Chem Commun. 148(July 2022). https://doi.org/10.1016/j.inoche.2022.110321

Mahieddine A, Adnane-amara L (2023) Constructing and electrochemical performance of NiCo-LDHs@h-Ni NWs core-shell for hydrazine detection in environmental samples. J Electroanal Chem 117168. https://doi.org/10.1016/j.jelechem.2023.117168

Masindi V, Muedi KL (2018) Environmental contamination by heavy metals. In: Saleh HEDM, Aglan RF (eds) Heavy Metals. IntechOpen, pp 115–133. https://doi.org/10.5772/intechopen.76082

Nodehi M, Baghayeri M, Kaffash A (2022) Application of BiNPs/MWCNTs-PDA/GC sensor to measurement of Tl (1) and Pb (II) using stripping voltammetry. Chemosphere 301:134701. https://doi.org/10.1016/j.chemosphere.2022.134701

Nodehi M, Baghayeri M, Veisi H (2021) Preparation of GO/Fe3O4@PMDA/AuNPs nanocomposite for simultaneous determination of As^{3+} and Cu^{2+} by stripping voltammetry. Talanta. 230(February):122288. https://doi.org/10.1016/j.talanta.2021.122288

Rahm CE, Torres-Canas F, Gupta P, Poulin P, Alvarez NT (2020) Inkjet printed multi-walled carbon nanotube sensor for the detection of lead in drinking water. Electroanalysis 32(2020):1533–1545

Palisoc S, Gonzales AG, Pardilla A, Racines L, Natividad M (2019) (2019) Electrochemical detection of lead and cadmium in UHT-processed milk using bismuth nanoparticles/Nafion®-modified pencil graphite electrode. Sens Bio-Sensing Res 23:100268

Phal S, Nguyễn H, Berisha A, Tesfalidet S (2021) (2021) In situ Bi/carboxyphenyl-modified glassy carbon electrode as a sensor platform for detection of Cd^{2+} and Pb^{2+} using square wave anodic stripping voltammetry. Sens Bio-Sens Res 34:100455

Safaei M, Beitollahi H, Shishehbore MR, Tajik S, Hosseinzadeh R (2019) Electrocatalytic determination of captopril using a carbon paste electrode modified with N-(ferrocenyl-methylidene) fluorene-2-amine and graphene/ZnO nanocomposite. J Serbian Chem Soc 84(2):175–185. https://doi.org/10.2298/JSC180414095S

Song HJ, Zhang LC, He CL, Qu Y, Tian YF, Lv Y (2011) (2011) Graphene sheets decorated with SnO_2 nanoparticles: in situ synthesis and highly efficient materials for cat luminescence gas sensors. J Mater Chem 21:5972

Sun W, Hong Y, Li T et al (2023) Biogenic synthesis of reduced graphene oxide decorated with silver nanoparticles (rGO/Ag NPs) using table olive (olea europaea) for efficient and rapid catalytic reduction of organic pollutants. Chemosphere 310(July 2022):136759. https://doi.org/10.1016/j.chemosphere.2022.136759

Sun YF, Wang J, Li PH, Yang M, Huang XJ (2019) Highly sensitive electrochemical detection of Pb(II) based on excellent adsorption and surface Ni(II)/Ni(III) cycle of porous flower-like NiO/rGO nanocomposite. Sens Actuators B 292(2019):136–147

Suvith VS, Devu VS, Philip D (2020) (2020) Facile synthesis of SnO2/NiO nano-composites: Structural, magnetic and catalytic properties. Ceram Int 46(1):786–794

Tabti S, Benchettara A, Smaili F, Benchettara A, Berrabah SE (2022) Electrodeposition of lead dioxide on Fe electrode: application to the degradation of Indigo Carmine dye. J Appl Electrochem 52(2022):1207–1217

Terbouche A, Lameche S, Ait-Ramdane-Terbouche C, Guerniche D, Lerari D, Bachari K, Hauchard D (2016) A new electrochemical sensor based on carbon paste electrode/Ru(III) complex for determination of nitrite: electrochemical impedance and cyclic voltammetry measurements. Measurement 92(2016):524–533

Vallee BL, Ulmer DD (1972) Biochemical effects of mercury, cadmium, and lead. Annu Rev Biochem 41(1972):91–128

Vorokhta M, Khalakhan I, Vondráček M, Tomeček D, Vorokhta M, Marešová E, Nováková J, Vlček J, Fitl P, Novotný M, Hozák P, Lančok J, Vrňatac M, Matolínová I, Matolín V (2018) Investigation of gas sensing mechanism of SnO_2 based chemiresistor using near ambient pressure XPS. Surf Sci 677(2018):284–290

Wang X, Xu M, Liu L, Cui Y, Geng H, Zhao H, Liang B, Yang J (2019) Effects specific surface area and oxygen vacancy on the photocatalytic properties of mesoporous F doped SnO_2 nanoparticles prepared by hydrothermal method. Jornl Matrl Scin Matrl in Elec 30(2019):16110–16123

Wei Y, Kong LT, Yang R, Wang L, Liu JH, Huang XJ (2011) Electrochemical impedance determination of polychlorinated biphenyl using a pyrenecyclodextrin-decorated single-walled carbon nanotube hybrid. Chem Commun 47(18):5340–5342. https://doi.org/10.1039/c1cc11267h

Wu Y, Pang H, Liu Y, Wang X, Yu S, Fu D, Chen J, Wang X (2019) Environmental remediation of heavy metal ions by novel-nanomaterials: a review. Environ Pollut 246(2019):608–620

Xu F, Deng M, Li G, Chen S, Wang L (2013) (2013) Electrochemical behavior of cuprous oxide–reduced graphene oxide nanocomposites and their application in nonenzymatic hydrogen peroxide sensing. Electrochim Acta 88:59

Zhang W, Fan S, Li X, Liu S, Duan D, Leng L, Cui C, Qu L (2020) Electrochemical determination of lead(II) and copper(II) by using phytic acid and polypyrrole functionalized metalorganic frameworks. Microchim Acta 187(2020):69–77

Zhang Z, Zhai S, Wang M, He L, Peng D, Liu S, Yang Y, Fang S, Zhang H (2015) (2015) Electrochemical sensor based on a polyaniline-modified SnO2 nanocomposite for detecting ethephon. Anal Method 7:4725

Zhou SF, Han XJ, Fan HL, Huang J, Liu YQ (2018) enhanced electrochemical performance for sensing Pb(II) based on graphene oxide incorporated mesoporous MnFe2O4 nanocomposites. J Alloys Compd 747(2018):447–454

Ziyatdinova G, Yakupova E, Davletshin R (2021) Voltammetric determination of hesperidin on the electrode modified with SnO_2 nanoparticles and surfactants. Electroanalysis 33(12):2417–2427. https://doi.org/10.1002/elan.202100405

Publisher's note Springer Nature remains neutral with regard to jurisdictional claims in published maps and institutional affiliations.

Springer Nature or its licensor (e.g. a society or other partner) holds exclusive rights to this article under a publishing agreement with the author(s) or other rightsholder(s); author self-archiving of the accepted manuscript version of this article is solely governed by the terms of such publishing agreement and applicable law.